Magnetic Resonance Materials in Physics, Biology and Medicine (2020) 33:507–513
https://doi.org/10.1007/s10334-019-00823-6

RESEARCH ARTICLE

Development of a new phantom simulating extracellular space of tumor cell growth and cell edema for diffusion-weighted magnetic resonance imaging

Ryoji Mikayama[1] · Hidetake Yabuuchi[2] · Ryoji Matsumoto[3] · Koji Kobayashi[3] · Yasuo Yamashita[3] · Mitsuhiro Kimura[1] · Takeshi Kamitani[4] · Koji Sagiyama[4] · Yuzo Yamasaki[4]

Received: 31 August 2019 / Revised: 7 December 2019 / Accepted: 19 December 2019 / Published online: 3 January 2020

Abstract

Objective A phantom for diffusion-weighted imaging is required to standardize quantitative evaluation. The objectives were to develop a phantom simulating various cell densities and to evaluate repeatability.

Materials and methods The acrylic fine particles with three different diameters were used to simulate human cells. Four-degree cell density components were developed by adjusting the volume of 10-μm particles (5, 20, 35, and 50% volume, respectively). Two-degree components to simulate cell edema were also developed by adjusting the diameter without changing number (17% and 40% volume, respectively). Spearman's rank correlation coefficient was used to find a significant correlation between apparent diffusion coefficient (ADC) and particle density. Coefficient of variation (CV) for ADC was calculated for each component for 6 months. A p value < 0.05 represented a statistically significance.

Results Each component (particle ratio of 5, 17, 20, 35, 40, and 50% volume, respectively) presented ADC values of 1.42, 1.30, 1.30, 1.12, 1.09, and 0.89 ($\times 10^{-3}$ mm^2/s), respectively. A negative correlation ($r = -0.986$, $p < 0.05$) was observed between ADC values and particle ratio. CV for ADC was less than 5%.

Discussion A phantom simulating the diffusion restriction correlating with cell density and size could be developed.

Keywords Diffusion-weighted imaging · Apparent diffusion coefficient · Standardized phantom · Tumor cell growth · Cell edema

Abbreviations

DWI Diffusion-weighted imaging
ADC Apparent diffusion coefficient
CV Coefficient of variation
SD Standard deviation

✉ Hidetake Yabuuchi
h-yabu@med.kyushu-u.ac.jp

Ryoji Mikayama
mikayama@r-tec.med.kyushu-u.ac.jp

Ryoji Matsumoto
r-matsu@r-tec.med.kyushu-u.ac.jp

Koji Kobayashi
kokoba@med.kyushu-u.ac.jp

Yasuo Yamashita
yasuo-y@med.kyushu-u.ac.jp

Mitsuhiro Kimura
mitsuhirokimura0426@gmail.com

Takeshi Kamitani
kamitani@radiol.med.kyushu-u.ac.jp

Koji Sagiyama
sagiyama@radiol.med.kyushu-u.ac.jp

Yuzo Yamasaki
yyama@radiol.med.kyushu-u.ac.jp

[1] Department of Health Sciences, Graduate School of Medical Sciences, Kyushu University, 3-1-1, Maidashi, Higashi-ku, Fukuoka, Fukuoka 812-8582, Japan

[2] Department of Health Sciences, Faculty of Medical Sciences, Kyushu University, 3-1-1, Maidashi, Higashi-ku, Fukuoka, Fukuoka 812-8582, Japan

[3] Division of Radiological Technology, Department of Medical Technology, Kyushu University Hospital, 3-1-1, Maidashi, Higashi-ku, Fukuoka, Fukuoka 812-8582, Japan

[4] Department of Clinical Radiology, Graduate School of Medical Sciences, Kyushu University, 3-1-1, Maidashi, Higashi-ku, Fukuoka, Fukuoka 812-8582, Japan

Introduction

Diffusion-weighted imaging (DWI) signal reflects the degree of water molecule diffusion in living tissue. The water molecule diffusion might considerably relate to the cellularity; therefore, DWI could detect early biological abnormality at the cellular level. DWI is one of the essential techniques for detecting various diseases, such as acute cerebral infarction, neoplasm, and inflammation [1–3]. It may also quantitatively evaluate lesions with apparent diffusion coefficient (ADC) values. The ADC reflects quantitative diffusivity of protons in biological tissues, and it could be modulated by the tissue structure including the presence of macromolecules. It is useful for tumor characterization as well as for predicting or monitoring the treatment response and prognosis [4]. The reproducibility of DWI is necessary for comparing the temporal change in monitoring the treatment response. Moreover, it is important to constantly provide similar information at different institutions using various equipment to realize clinical utility of ADC among multiple institutions [4]; however, ADC may differ among the vendors, field strengths, sequences, and imaging centers because the image acquisition method of DWI has not been standardized [5–9]. In these studies, the volunteers or self-developing phantoms were used as specimens because a phantom dedicated to DWI was not established. Therefore, a standardized phantom for DWI is required to establish the basic standard for quantitative evaluation of tissue diffusion. In most cases, DWI phantoms have been created by adjusting the viscosity using agarose, sucrose, gelatin, polyethylene glycol, and polyvinylpyrrolidone, or by modulating the Brownian motion to control water temperature [10–15]. These simple fluid-based test objects can be easily created; however, it is difficult to store them for a longer time. To the best of our knowledge, no phantoms have simulated the restriction to water displacement depending on the difference in the extracellular space. Therefore, the purposes of our study were to develop a phantom simulating various extracellular spaces and to evaluate their DWI reproducibility.

Materials and methods

Acrylic fine particle/detergent

We hypothesized that we would be able to simulate the restricted water mobility for decreasing extracellular space using acrylic fine particles. There are numerous types of cells in human tissues varying in sizes. For example, in a Monte Carlo study of diffusion models of varying microstructural environments, typical human cell size were specified to have a 10 μm diameter [16]. Therefore, the insoluble polymethyl methacrylate particles with mean diameters of 10 μm were adopted to simulate human cells based on their size. The detergent was used for uniform dispersion of these particles.

Twelve pilot phantom components were prepared to simulate the reduction of ADC due to the change in extracellular space by adjusting the acrylic fine particles and viscosity using the detergent diluted with purified water. In six of these components, the acrylic fine particles varied from 5 to 50%, whereas the detergent concentration was kept at 33%. In other six components, the detergent concentration varied from 20 to 100%, whereas the acrylic fine particles were not used. After packing all phantom components in the container, the pilot phantom was stored in the MR examination room at a controlled temperature of 24–25 °C because the water molecular mobility was dependent on the temperature [14].

Diffusion phantom

In developing the phantom, the acrylic fine particles with diameters of three grades (10, 15, and 20 μm) were used to simulate human cells. About 110-mL vials with 40 mm diameter and 120 mm height were chosen as containers for each phantom component. First, we prepared four grades of extracellular space phantoms simulating the various degrees of the tumor cell growth by adjusting the 10-μm particle counts (5%, 20%, 35%, and 50% particle volume ratio), which were dispersed in the detergent diluted with purified water (Fig. 1). Second, two grade cell size phantoms were developed to simulate the cell edema. In each phantom, 15- and 20-μm particles were dispersed (17% and 40% particle volume ratio) in the detergent diluted with purified water without changing the particle counts to 5% volume ratio of 10-μm particles (Fig. 1). All phantom components were packed in a polypropylene cylindrical container filled with water, with 184 mm diameter and 133 mm height. The concentration of the detergent was adjusted based on the results of the ADC decay curve presented in Fig. 2 to develop the phantom corresponding to the ADC about 1.0×10^{-3} mm^2/s as an index of discrimination between the benign and malignant tumors. The developed phantom was stored in the MR examination room at a controlled temperature of 24–25 °C. The phantom was shaken for 3 min to redisperse the particles and it was settled for 5 min on the scanner before each MR imaging.

MR imaging protocol

MR examinations were performed on a 3 T MR scanner (Intera Achieva 3.0 T TX, Philips Healthcare, Best, The

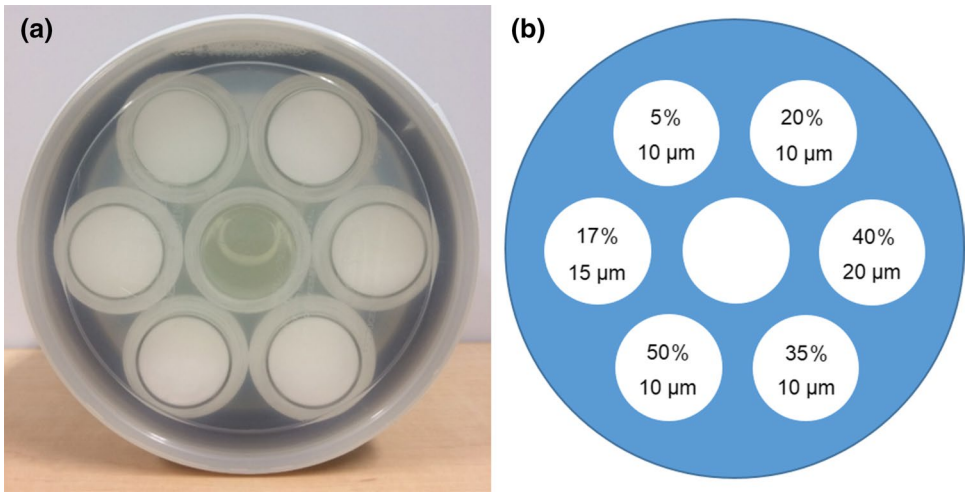

Fig. 1 The developed diffusion phantom (**a**), and cross section of the spherical diffusion phantom (**b**). The percentages present the particle ratio, and the particle size is given in μm

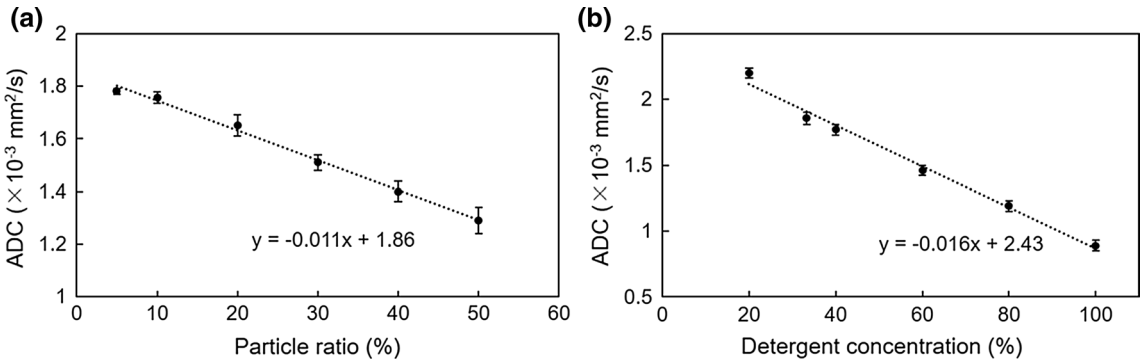

Fig. 2 Linear regression analyses of particle ratio (**a**) and detergent concentration (**b**) versus the apparent diffusion coefficients (ADCs). Plots present the mean ADC and error bars indicate the ADC difference in the region of interest. The y functions in these equations reveal ADC, and x functions present the particle ratio (**a**) or detergent concentration (**b**). These were highly accurate fitting in restricted water mobility by increasing of particle ratio (R^2 = 0.992, p < 0.0001) and detergent concentration (R^2 = 0.990, p = 0.0004)

Netherlands) with an eight-channel-SENSE head coil. The developed phantom was set on the scanner bed at the z-axis of the magnet for axial imaging. It was scanned every month, and the examination during the 3rd month was defined as the end point for confirming the three-term reproducibility. In addition, the 6th month was defined as the end point for confirming the long-term reproducibility. Each examination was performed in repetition of six times to minimize the internal error of the scanner. DWI was performed using a single-shot spin-echo echo-planar imaging with four b values (b = 0, and 1000 s/mm^2) and following parameters: TR = 6000 ms, TE = 62 ms, field of view = 300 × 300 mm, acquisition matrix = 208 × 165, reconstruction matrix = 336 × 336, number of average = 1, sensitivity encoding reduction factor = 2.5, bandwidth in frequency direction = 2033.6 Hz/pixel, spectral attenuated inversion recovery for fat suppression, slice thickness = 5 mm, slice gap = 1 mm, number of slice = 18, and scan time = 2 min 12 s. The long TR and short TE were set because an error was produced in the ADC by setting a short TR or a long TE for a material with long T1 and short T2 value [17].

We simultaneously calculated ADC values of a water tube to secure the temporal stability of MR scanner for the ADC measurement at each examination.

Data analysis

ADC maps were automatically generated from diffusion-weighted images at b values of 0 and 1000 s/mm^2 on a pixel-by-pixel basis using Synapse Vincent (Fujifilm Medical, Tokyo, Japan). To calculate the average ADC, one radiologist manually set the circular regions of interest of 20 pixel diameter on the center of each phantom component avoiding the artifacts (Fig. 3c). The ADC of water filled in container was also measured to confirm the temporal change of scanner. We calculated the average value of ADC from the central six slices at each examination for each examination time point.

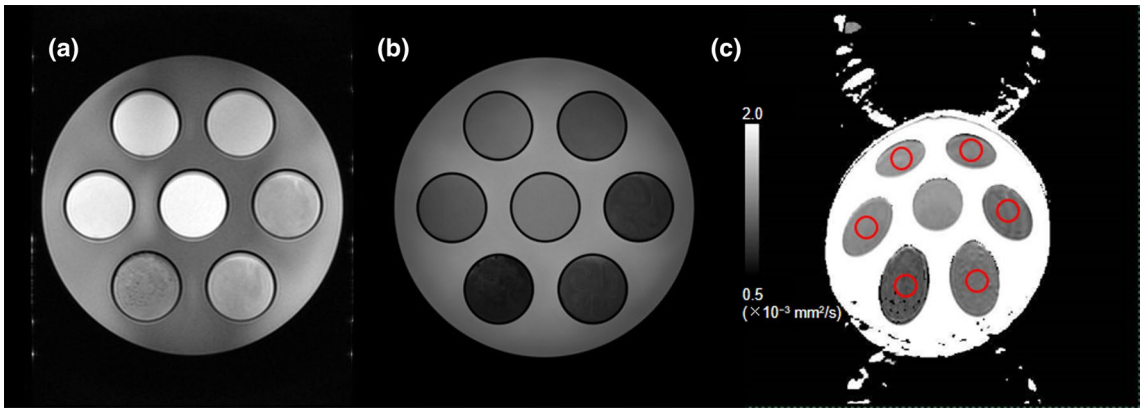

Fig. 3 Diffusion-weighted image of $b=0$ s/mm^2 (**a**), $b=1000$ s/mm^2 (**b**), and apparent diffusion coefficient (ADC) map (c) for the developed phantom. ADC map was generated from images acquired with the echo-planar imaging (EPI)-based diffusion-weighted imaging protocol, described in "Materials and methods". ADC values were measured at regions of interest (red circles) on the center of each phantom component

The microscopic observations of 10-, 15-, and 20-μm acrylic particles were performed before and after MR acquisition of the phantom. We put the unused acrylic particles and those used 6 months after for phantom in the middle of microscope preparation with detergent of 60% concentration and inserted an objective micrometer of 50 μm. We finally put cover glass over them to avoid the mixture of air bubbles. One radiologist captured five views of the microscopic images at each preparation using Nikon Eclipse NI-U microscope (Nikon, Tokyo, Japan) at a magnification of 400, and the diameters of all acrylic fine particles were measured using ImageJ (National Institutes of Health, Bethesda, MD, USA).

Statistical analysis

Linear regression analysis was performed to evaluate the correlation between the ADC and particle ratio or detergent concentration in the pilot phantom. Regression lines were calculated by linear approximation using the least square method. Spearman's rank correlation coefficient was evaluated to test whether a significant correlation existed between the ADC and particle ratio in developed diffusion phantom. The coefficient of variance (CV) was calculated for each phantom component using the same set of measurement every month. The CV was the percentage of standard deviation (SD)/mean, and was used to verify the temporal stability of the diffusion properties in the developed phantom. The normal distribution of diameters of the acrylic particles was tested using the Shapiro–Wilk test. Thereafter, the mean diameters of the acrylic fine particles before and after use were compared using a two-sample two-tailed t test when the data were normally distributed. All statistical analyses were performed using JMP Pro 11.0.0 software (SAS Institute, Cary, NC, USA). A p value <0.05 represented statistically significant difference.

Results

Restricted water mobility by acrylic fine particle and detergent

Figure 2a, b presents the linear regression analysis of ADC values according to the diffusion properties on the particle ratio and detergent concentration for the pilot phantom. These were highly accurate, fitting in the restricted water mobility by particle ratio ($R^2=0.992$, $p<0.0001$) and detergent concentration ($R^2=0.990$, $p=0.0004$).

The ADC of the developed phantom

The detergent with 60% concentration was adopted for the developed phantom on the basis of the present study results (Fig. 2). The DWI ($b=0$ and 1000 s/mm^2) and ADC map for the developed phantom are presented in Fig. 3. Each phantom component at tumor cell growth model (particle ratio of 5, 20, 35, and 50% volume, respectively) exhibited the mean ADC of 1.42 ± 0.03, 1.30 ± 0.04, 1.12 ± 0.03, and 0.89 ± 0.05 ($\times10^{-3}$ mm^2/s), respectively, whereas those at cell edema model (particle size of 10, 15, and 20 μm, respectively) presented mean ADC of 1.42 ± 0.03, 1.30 ± 0.03, and 1.09 ± 0.03 ($\times10^{-3}$ mm^2/s), respectively. There was a strong negative correlation ($r=-0.986$, $p<0.05$) between the ADC and particle ratio (Fig. 4).

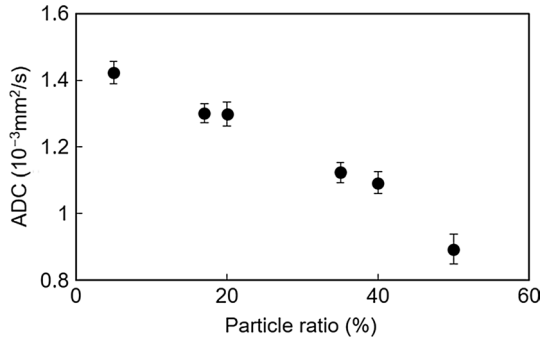

Fig. 4 The apparent diffusion coefficient (ADC) of each particle ratio of the developed phantom. There was a strong negative correlation ($r = -0.986$, $p < 0.05$) between ADC and particle ratio

The temporal stability of the developed phantom

At first, we confirmed the temporal stability of the MR scanner to evaluate ADC values. The ADC of a water tube showed a small variation within CVs of 1.5%. The temporal stability of the diffusion properties of the developed phantom was assessed over a middle term for 3 months. The temporal variations of ADC for all the phantom components at the tumor cell growth and cell edema models are presented in Fig. 5. The CV for ADC of the developed phantom is presented in Table 1. Tumor cell growth model (particle ratio of 5%, 20%, 35%, and 50% volume) at each phantom component revealed a CV of 2.2%, 2.5%, 1.3%, and 3.6%, respectively, and cell edema model (particle size of 10, 15, and 20 μm) presented CV of 2.2%, 1.9%, and 0.9%, respectively. The long-term stability of the developed phantom was also assessed after 6 months. Tumor cell growth model (particle ratio of 5, 20, 35, and 50% volume) at each phantom component presented mean ADC of 1.40 ± 0.03, 1.29 ± 0.03, 1.14 ± 0.02, and 0.99 ± 0.04 ($\times 10^{-3}$ mm^2/s), respectively, and the cell edema model (particle size of 10, 15, and 20 μm) revealed ADC of 1.40 ± 0.03, 1.30 ± 0.02, and 1.13 ± 0.04 ($\times 10^{-3}$ mm^2/s), respectively, after 6 months. In the particle ratio of 50% volume, the ADC changed from 0.89×10^{-3} mm^2/s at 0 month to 0.99×10^{-3} mm^2/s after 6 months. In the other phantom components, no noticeable change was observed.

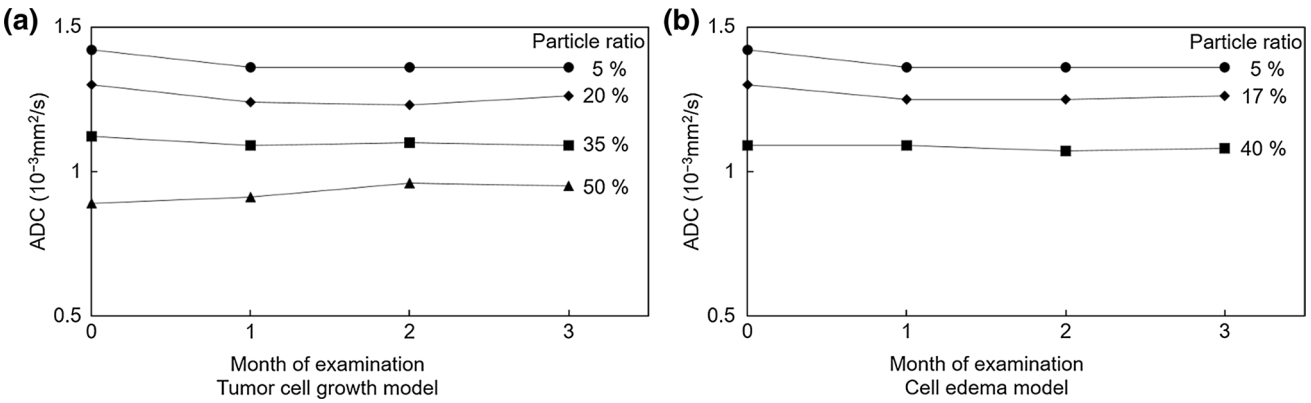

Fig. 5 The temporal stability of diffusion properties of the developed phantom components for 3 months. In the tumor cell growth model (**a**), round, rhombus, square, and triangular plots present the apparent diffusion coefficient (ADC) of 5%, 20%, 35%, and 50% particle ratio phantoms, respectively. In the cell edema model (**b**), round, rhombus, and square plots present the ADC of 5%, 17%, and 40% particle ratio phantoms, respectively (10, 15, and 20 μm particles, respectively)

Table 1 The CV of the ADC value in tumor cell growth model and cell edema model for 3 months

Model	Particle ratio (diameter)	0 month	1 month	2 months	3 months	CV (%)
Tumor cell growth	5% (10 μm)	1.42 ± 0.03	1.36 ± 0.03	1.36 ± 0.04	1.36 ± 0.03	2.18
	20% (10 μm)	1.30 ± 0.04	1.24 ± 0.03	1.23 ± 0.04	1.26 ± 0.05	2.46
	35% (10 μm)	1.12 ± 0.03	1.09 ± 0.03	1.10 ± 0.04	1.09 ± 0.05	1.29
	50% (10 μm)	0.89 ± 0.05	0.91 ± 0.07	0.96 ± 0.06	0.95 ± 0.06	3.56
Cell edema	5% (10 μm)	1.42 ± 0.03	1.36 ± 0.03	1.36 ± 0.04	1.36 ± 0.03	2.18
	17% (10 μm)	1.30 ± 0.03	1.25 ± 0.02	1.25 ± 0.04	1.26 ± 0.04	1.89
	40% (10 μm)	1.09 ± 0.03	1.09 ± 0.03	1.07 ± 0.03	1.08 ± 0.06	0.88

Data are means ± standard deviations

CV coefficient of variation

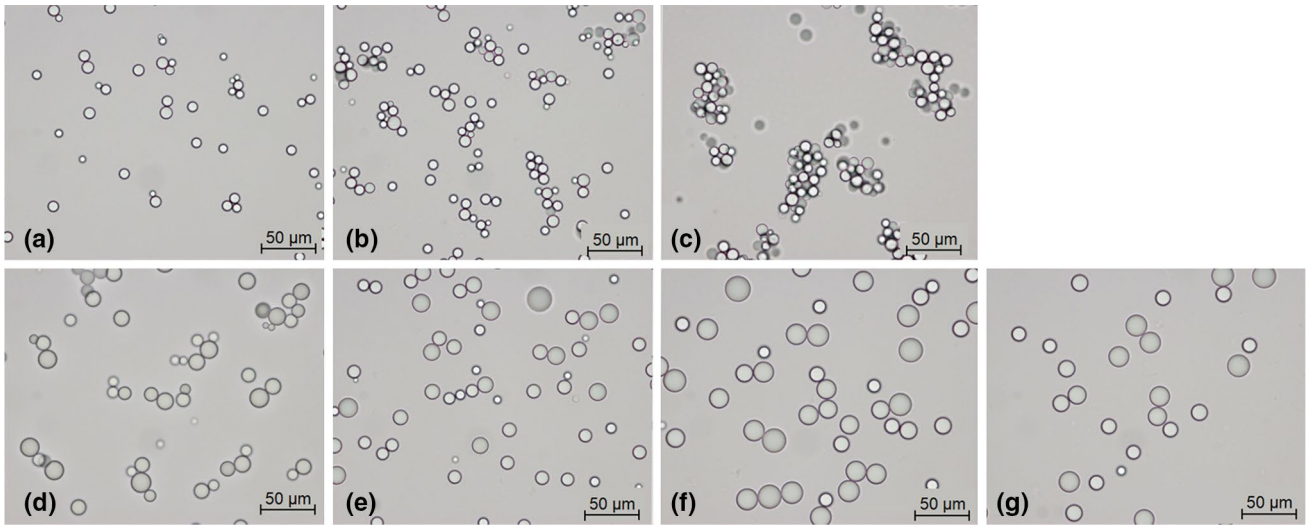

Fig. 6 The microscopic images (original magnification, × 400) of 10-μm acrylic particles before use (**a**), 10-μm acrylic particles after use at 5% particle ratio (**b**), 10-μm acrylic particles after use at 50% particle ratio (**c**), 15-μm acrylic particles before use (**d**), 15-μm acrylic particles after use at 17% particle ratio (**e**), 20-μm acrylic particles before use (**f**), and 20-μm acrylic particles after use at 40% particle ratio (**g**). In 10-μm particle of 50% volume ratio, the acrylic fine particles were assembled together

Table 2 The diameters of acrylic particles before and after use

Particle size (μm)	Before use	After use	*p* value
10	8.28 ± 1.6	8.12 ± 1.9	0.27
15	12.1 ± 2.6	11.8 ± 3.0	0.28
20	15.9 ± 3.5	15.4 ± 3.3	0.28

Data are means ± standard deviations

The presence of any morphological change in the acrylic fine particles was verified with a microscope. The microscopic images are presented in Fig. 6. The mean diameters of the acrylic particles were as follows: 10 μm before use, 8.28 ± 1.6 μm; 10 μm after use, 8.12 ± 1.9 μm; 15 μm before use, 12.1 ± 2.6 μm; 15 μm after use, 11.8 ± 3.0 μm; 20 μm before use, 15.9 ± 3.5 μm; and 20 μm after use, 15.4 ± 3.3 μm. As presented in Table 2, no significant change was observed between the diameter of acrylic fine particles before and after use. In 10-μm particle of 50% volume ratio, the acrylic fine particles were aggregated together (Fig. 6b).

Discussion

Our study results indicate that the ADC decreased with the increase in the particle ratio (Fig. 4). Brownian motion was supposed to be restricted by the presence of acrylic fine particles as barriers to diffusion within the water microenvironment. The regions with small extracellular space had lower ADC than those with large extracellular space [18]. Therefore, the acrylic fine particles presented in this study could simulate the tumor extracellular space. In the developed phantom, a strong correlation was observed between the ADC and particle ratio (Fig. 4). The cell membranes significantly contribute as the diffusion barriers in living tissues. A previous report has examined the relationship between ADC and extracellular space at lesions in vivo; however, viable tumor involved various factors such as organelles, fibers, and soluble macromolecules [18]. Therefore, the ADC reduction caused by only the scarce extracellular space could be simulated in this study.

In this MR scanner, the DWI repeatability was confirmed because the water ADC showed a small variation with a CV of 1.5%. CV for the ADC stability measurements in all phantom components for 3 months was less than 5%. No significant differences were observed in the diameters of acrylic fine particles over 3 months during the microscopic investigation. These results indicated that no significant change was observed in the physical properties of the acrylic fine particles due to water absorption or denaturation. Nevertheless, in the particle ratio of 50% volume, the ADC increased by about 10% after 6 months. The increase in ADC at 50% volume particle ratio resulted from the reduced surface area of the acrylic fine particles by self-aggregation (Fig. 6b). This phantom simulating extracellular space was available as a standardized material for DWI except for the phantom component of 50% volume particle ratio.

This study had four limitations. First, our study used only one MRI unit of only one manufacturer. It is necessary to confirm whether our developed phantom shows similar relationships between the ADC and the density of acrylic particles in MR unit of other manufacturers. Second, the

acrylic fine particles used in this study could not simulate the human cell completely. The insoluble acrylic fine particles were precipitated over time because the density of the particle was 1.2 g/cm^3. To disperse the acrylic fine particles, developed phantom was shaken before scanning. In contrast, the actual human cells cannot float; therefore, this difference might influence the ADC measurements. Nevertheless, we confirmed that there were no sedimentation of particles after each DWI scanning. Accordingly, this phantom might be unsuitable for qualitative analysis because acrylic fine particles had no MR signal. Third, developed phantom simulated only extracellular diffusion. In the living tissue, water diffusion was limited to both the extracellular and intracellular elements [19]. Moreover, the capillary blood flow might be mistakenly attributed to living tissue diffusion [20]. Accordingly, this phantom could partly simulate the diffusivity of living tissue. Forth, we presented a DWI phantom simulating extracellular spaces; However, it was not compared to in vivo images and the reachable ADC range was limited since aggregation of particles was visible in the higher density volumes. Future work should develop a DWI phantom completely simulating intra- and extra-cellular diffusion reproducing sufficient in vivo range of fluctuation of extracellular spaces.

In conclusion, a phantom simulating restricted water mobility, correlating with the reduction of extracellular space caused by tumor cell growth and cell edema, could be developed using acrylic fine particles, and reproducibility could also be confirmed. The developed phantom is a promising tool to evaluate the use of DWI and ADC measurement of the effect of extracellular restricted water diffusion.

Author contributions Study conception and design: HY. Acquisition of data: RM, HY, RM, KK, and YY. Analysis and interpretation of data: RM, HY, and MK. Drafting of manuscript: RM. Critical revision: HY, TK, KS, and YY.

Compliance with ethical standards

Conflict of interest The authors declare that they have no conflict of interest.

Ethical approval This article does not contain any studies with human participants performed by any of the authors.

References

1. Schaefer PW, Grant PE, Gonzalez RG (2000) Diffusion-weighted MR imaging of the brain. Radiology 217:331–345
2. Tien RD, Felsberg GJ, Friedman H, Brown M, MacFall J (1994) MR imaging of high-grade cerebral gliomas: value of diffusion weighted echo planar pulse sequences. AJR 162:671–677
3. Okamoto K, Ito J, Ishikawa K, Sakai K, Tokiguchi S (2000) Diffusion-weighted echo-planar MR imaging in differentiation diagnosis of brain tumors and tumor-like conditions. Eur Radiol 10:1342–1350
4. Koh DM, Collins DJ (2007) Diffusion-weighted MRI in the body: applications and challenges in oncology. AJR 188:1622–1635
5. Kolff-Gart AS, Pouwels PJW, Noji DP et al (2015) Diffusion-weighted imaging of the head and neck in healthy subjects: reproducibility of ADC values in different MRI systems and repeat sessions. AJNR 36:384–390
6. Braithwaite AC, Dale BM, Boll DT, Merkle EM (2009) Short- and midterm reproducibility of apparent diffusion coefficient measurements at 3.0-T diffusion-weighted imaging of the abdomen. Radiology 250:459–465
7. Kivrak AS, Paksoy Y, Erol C, Koplay M, Ozbek S, Kara F (2013) Comparison of apparent diffusion coefficient values among different MRI platforms: a multicenter phantom study. Diagn interv Radiol 19:433–437
8. Sasaki M, Yamada K, Watanabe Y et al (2008) Variability in absolute apparent diffusion coefficient values across different platforms may be substantial: a multivendor, multi-institutional comparison study. Radiology 249:624–630
9. Malyarenko DI, Newitt D, Wilmes LJ et al (2016) Demonstration of nonlinearity bias in the measurement of the apparent diffusion coefficient in multicenter trials. Magn Reson Med 75:1312–1323
10. Lavdas I, Behan KC, Papadaki A, McRobbie DW, Aboagye EO (2013) A phantom for diffusion-weighted MRI (DW-MRI). J Magn Reson Imaging 38:173–179
11. Matsuya R, Kuroda M, Matsumoto Y et al (2009) A new phantom using polyethylene glycol as an apparent diffusion coefficient standard for MR imaging. Int J Oncol 35:893–900
12. Gatidis S, Schmidt H, Martirosian P, Schwenzer NF (2014) Development of an MRI phantom for diffusion-weighted imaging with independent adjustment of apparent diffusion coefficient values and T2 relaxation times. Magn Reson Med 72:459–463
13. Chenevert TL, Galban CJ, Ivancevic MK et al (2011) Diffusion coefficient measurement using a temperature-controlled fluid for quality control in multicenter studies. J Magn Reson Imaging 34:983–987
14. Malyarenko D, Galban CJ, Londy FJ et al (2013) Multi-system repeatability and reproducibility of apparent diffusion coefficient measurement using an ice-water phantom. J Magn Reson Imaging 37:1238–1246
15. Jerome NP, Papoutsaki MV, Orton MR et al (2016) Development of a temperature-controlled phantom for magnetic resonance quality assurance of diffusion, dynamic, and relaxometry measurements. Med Phys 43:2998–3007
16. Lee CY, Bennett KM, Debbins JP (2013) Sensitivities of statistical distribution model and diffusion kurtosis model in varying microstructural environments: a Monte Carlo study. J Magn Reson 320:19–26
17. Ogura A, Hayakawa K, Miyati T, Maeda F (2011) Imaging parameter effects in apparent diffusion coefficient determination of magnetic resonance imaging. Eur J Radiol 77:185–188
18. Lyng H, Haraldseth O, Rofstad EK (2000) Measurement of cell density and necrotic fraction in human melanoma xenografts by diffusion weighted magnetic resonance imaging. Magn Reson Med 43:828–836
19. Szafer A, Jianhui Z et al (1995) Theoretical model for water diffusion in tissues. Magn Reson Med 33:697–712
20. Le Bihan D, Breton E, Lallemand D, Aubin ML, Vignaud J, Laval-Jeantet M (1988) Separation of diffusion and perfusion in intravoxel incoherent motion MR imaging. Radiology 168:497–505